

1 **Effects of changes in moisture source and the upstream rainout on stable**
2 **isotopes in precipitation — a case study in Nanjing, East China**

3
4 Yanying Tang¹, Hongxi Pang^{1,2*}, Wangbin Zhang¹, Yaju Li¹, Shuangye Wu^{1,3}, Shugui Hou^{1,2*}

5 1.Key Laboratory of Coast and Island development of Ministry of Education, School of
6 Geographic and Oceanographic Sciences, Nanjing University, Nanjing 210023, China;

7 2.Collaborative Innovation Center of Climate Change, Jiangsu Province, China;

8 3.Geology Department, University of Dayton, Ohio 45469-2364, USA.

9 *Correspondence to: Hongxi Pang (hxpang@nju.edu.cn); Shugui Hou (shugui@nju.edu.cn)

10
11 **Abstract.** In the Asian monsoon region, variations in the stable isotopic composition of
12 speleothems have often been attributed to the “amount effect”. However, an increasing number
13 of studies suggest that the “amount effect” in local precipitation is insignificant or even
14 non-existent. To explore this issue further, we examined the variability of daily stable isotopic
15 composition ($\delta^{18}\text{O}$) in precipitation from September 2011 to November 2014 in Nanjing, East
16 China. We found that **intra-seasonal variations of $\delta^{18}\text{O}$ during summer** was not significantly
17 correlated with local rainfall amount, but could be linked to changes in the moisture source
18 location and rainout processes in the source regions. Our findings suggest that the stable isotopes
19 in summer precipitation could signal the location shift of precipitation source regions in the
20 inter-tropical convergence zone (ITCZ) over the course of the monsoon season. As a result,
21 changes in moisture source location and upstream rainout effect should be taken into account
22 when interpreting the stable isotopic composition of speleothems in the Asian monsoon region.

23 In addition, the temperature effect on isotopic variations in non-monsoonal precipitation should
24 also be considered because precipitation in the non-monsoon season accounts for about half of its
25 annual precipitation.

26

27 **1 Introduction**

28 The “amount effect” refers to the observed negative correlation between the isotopic
29 composition in precipitation and rainfall amount. It was first **proposed** by Dansgaard (1964), and
30 is generally observed in low-latitude regions (Araguás-Araguás et al., 1998). Based on this
31 relationship, stable isotopic records obtained from low-latitude regions are often used for
32 paleohydroclimate reconstructions (Cruz et al., 2005, 2009; Partin et al., 2007; Tierney et al.,
33 2008; Sano et al., 2012). However, some recent studies suggest that the “amount effect” is
34 insignificant or even non-existent in low-latitude monsoon areas. For example, Conroy et al.
35 (2013) found spatial and temporal examples of precipitation–isotope mismatches across the
36 tropical Pacific, indicating that factors beyond the “amount effect” influenced precipitation
37 isotope variability. They compared 12 isotope-equipped global climate models to assess the
38 distribution of simulated stable isotopic variability. Model simulations support observations in
39 the western tropical Pacific, showing that monthly $\delta^{18}\text{O}$ are correlated with large-scale, not local,
40 precipitation (Conroy et al., 2013). Peng et al. (2010) also found no significant correlation
41 between precipitation amount and $\delta^{18}\text{O}$ values in the western Pacific monsoon region near
42 Taiwan. They suggest that moisture sources of diverse air masses with different isotopic signals
43 are the main factor controlling the precipitation isotopic characteristics. Breitenbach et al. (2010)
44 observed no empirical amount effect at their study site in the monsoonal northeast India. They

45 identified a strong trend towards lighter isotope values over the course of the summer monsoon,
46 with lowest $\delta^{18}\text{O}$ and δD values in late monsoon season, and a temporal offset between the
47 highest rainfall and the most negative $\delta^{18}\text{O}$. Other observations (Lawrence et al., 2004; Kurita et
48 al., 2009) show that at marine island stations, even short-term (daily or event-based) isotopic
49 variations are independent of local precipitation intensity, but **are instead** linked to rainout
50 processes in the surrounding regions. Some ice core studies also suggest that records of
51 precipitation $\delta^{18}\text{O}$ in ice cores of the Indian monsoon region do not match the local precipitation
52 amount. For example, Pang et al. (2014) found a significant correlation between $\delta^{18}\text{O}$ records
53 from the East Rongbuk ice cores and summer monsoon rainfall along the southern slope of the
54 Himalayas, whereas no significant correlation was found between the $\delta^{18}\text{O}$ records and
55 accumulation rates (an indicator of local precipitation). This suggests that summer monsoon
56 precipitation $\delta^{18}\text{O}$ over the high Himalayas is controlled by the upstream rainout over the entire
57 southern slope of the Himalayas rather than local precipitation processes.

58 Stable oxygen isotopes in speleothems are widely used for paleoclimate reconstructions.
59 Recently, stable oxygen isotopes measured in cave speleothems from China have received much
60 attention: e.g., Hulu Cave (Wang et al., 2001), Dongge Cave (Yuan et al., 2004; Dykoski et al.,
61 2005; Kelly et al., 2006), Sanbao Cave (Wang et al., 2008; Cheng et al., 2009), Heshang Cave
62 (Hu et al., 2008), Wanxiang Cave (Zhang et al., 2008), Buddha Cave (Paulsen et al., 2003), and
63 Dayu Cave (Tan et al., 2009) (Fig. 1a). However, the interpretation of these stable isotope
64 records in speleothems remains controversial. Some researchers used the stable isotope records
65 from stalagmites in monsoonal east China as proxies for precipitation amount (Hu et al., 2008;
66 Tan et al., 2009; Cai et al., 2010). Paulsen et al. (2003) showed that short-term (<10 years)

67 variations in $\delta^{18}\text{O}$ in stalagmites from Buddha Cave reflect changes in precipitation amounts, but
68 longer-term (>50 years) $\delta^{18}\text{O}$ variations **are related to** changes in air temperature. Other studies
69 suggest that $\delta^{18}\text{O}$ indicates changes in the ratio of summer/winter precipitation, which they refer
70 to as “monsoon intensity” (Wang et al., 2001; Yuan et al., 2004; Dykoski et al., 2005; Kelly et al.,
71 2006; Wang et al., 2008; Zhang et al., 2008; Cheng et al., 2009). Dayem et al. (2010) reported
72 that annual and rainy season precipitation totals in each of central China, south China, and east
73 India have correlation length scales of ~500 km, shorter than the distance between many
74 speleothem records that share similar long-term time variations in $\delta^{18}\text{O}$ values. Thus, the short
75 correlation distances do not support the idea that apparently synchronous variations in $\delta^{18}\text{O}$
76 values at widely spaced (>500 km) caves in China are due to variations in annual precipitation
77 amounts. Most of the above-mentioned studies indicate that the variations of $\delta^{18}\text{O}$ in speleothems
78 from the Asian summer monsoon region are not controlled by the local precipitation amount.

79 Recent studies have revealed the importance of variability in moisture sources (Peng et al.,
80 2010; Xie et al., 2011) and large-scale convective activities (Vimeux et al., 2011; Tremoy et al.,
81 2012; Kurita, 2013; Moerman et al., 2013; Lekshmy et al., 2014; He et al., 2015) in controlling
82 precipitation $\delta^{18}\text{O}$ in monsoon regions. Strong convection at source regions tends to produce
83 more precipitation, causing heavy isotopes to preferentially condense from vapor, leading to
84 lower values of downstream precipitation $\delta^{18}\text{O}$. In addition, the location of moisture source
85 determines the distance that water vapor has to travel, hence affects the precipitation $\delta^{18}\text{O}$.
86 Soderberg et al. (2013) found that the variability of the isotopic composition of individual rain
87 events in central Kenya could be partly explained by the distance traveled by an air mass over
88 land. Therefore, the rainout effect at the water vapor source areas and upstream regions should

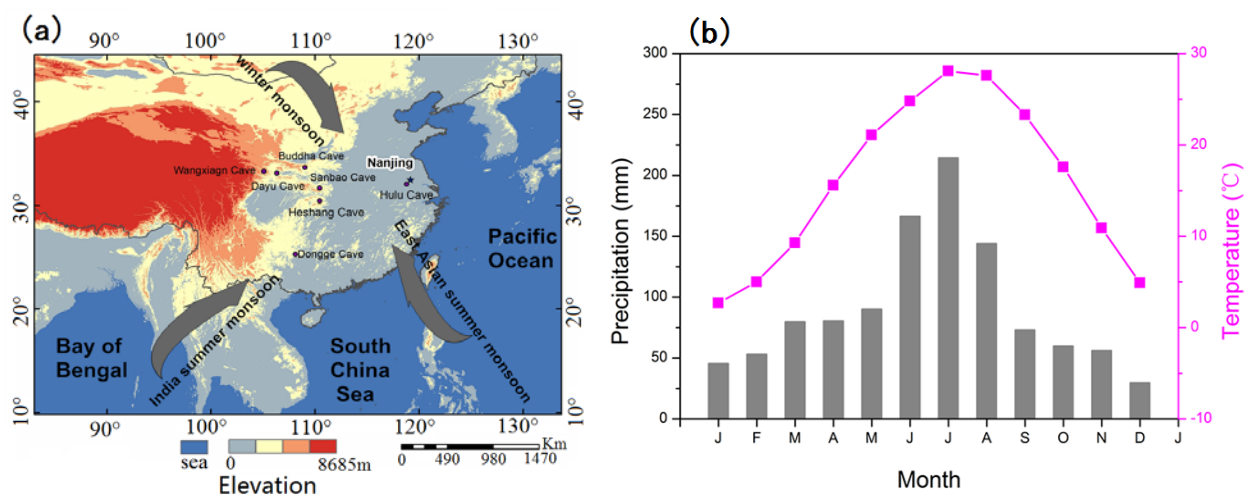
89 have a significant influence on stable isotopes in precipitation in downstream regions (Vuille et
90 al., 2005).

91 In the Asian monsoon regions, moisture sources for summer precipitation often lie in the
92 strong convection areas within the inter-tropical convergence zone (ITCZ). The variability of
93 ITCZ position and intensity could therefore affect precipitation $\delta^{18}\text{O}$ in these regions. Using the
94 outgoing longwave radiation (OLR) as a tracer for deep tropical convection (Wang et al., 1997),
95 the ITCZ position and strength **can** be identified (Gu and Zhang, 2002). In the East Asia–West
96 Pacific region, the onset of the Asian summer monsoon corresponds to the northward movement
97 of the ITCZ to an area 5° – 25°N (Ding, 2007), and brings with it large amounts of convective
98 precipitation (Ananthakrishnan et al., 1981). In this study, we focused on a detailed examination
99 of how summer precipitation $\delta^{18}\text{O}$ related to changes in the position and intensity of moisture
100 sources within ITCZ, using the daily $\delta^{18}\text{O}$ data at Nanjing in summer (June–September) during
101 2012–2014, the daily OLR data, and relevant meteorological data. However, according to long
102 term monthly means of Nanjing precipitation for the years 1981–2010 from the China
103 Meteorological Data Sharing Service System (<http://cdc.nmic.cn/home.do>), summer precipitation
104 (June–September) accounts for 54.8% of its annual precipitation, indicating that the
105 non-monsoonal precipitation (45.2%) (October–May) is also important. Therefore, factors
106 controlling the isotopic variations in the non-monsoonal precipitation **are** also discussed in order
107 to provide more observational basis for better interpretation of the oxygen isotopic records in
108 speleothems in the Asian monsoon region.

109

110 **2 Study area**

111 Nanjing is located on the lower reaches of the Yangtze River, surrounded by low hilly
 112 terrain with an average altitude of 26 m (Fig. 1a). The mean annual air temperature is 16°C and
 113 the average annual precipitation is 1106 mm. Located close to the Tropic of Cancer, this area has
 114 a strong seasonal climate (Fig. 1b), with a distinct seasonal reversal of wind and alternation of
 115 dry and rainy periods.



116 Fig. 1. (a) Elevation map of China; the study site Nanjing is marked by a black star. Black dots
 117 indicate the cave locations mentioned in this study: Hulu, Dongge, Heshang, Sanbao, Wanxiang,
 118 Buddha, and Dayu. Grey arrows indicate the dominant circulation patterns over the region in
 119 summer and winter. (b) Monthly average temperature and precipitation 1981–2010 at Nanjing
 120 (data from the China Meteorological Data Sharing Service System).
 121

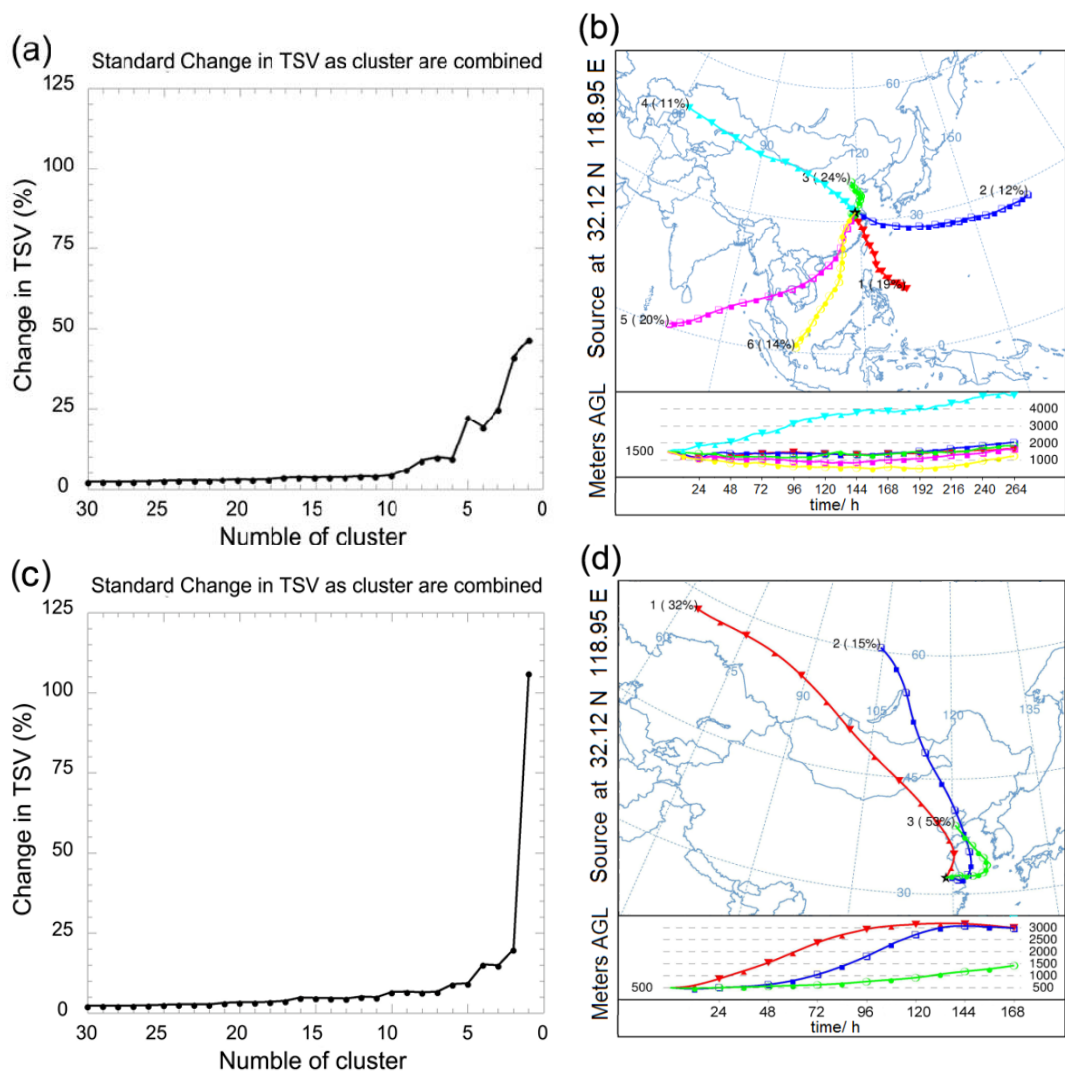
122

123 In the summer (June to September), the study area is under the influence of both the East
 124 Asian summer monsoon and the Indian summer monsoon (Fig. 1a). With the onset of the
 125 summer monsoon, the warm and moist air masses from the south collide with cold air masses
 126 from the north in eastern China, forming a quasi-stationary rain belt known as Meiyu, also
 127 known as Baiu in Japan (Saito, 1995) and Changma in Korea (Oh et al., 1997). Meiyu starts in

128 southern China between April and May, moving to the middle part of eastern China (Yangtze and
129 Huai He River Basins) between May and July, and to northern China between July and August,
130 bringing with it consistent rainfall (Ding et al., 2007). The vapor trajectories indicate that
131 moisture for summer precipitation at Nanjing mainly comes from the Bay of Bengal, the South
132 China Sea, and the western Pacific (Fig. 2b). Heavy water isotopes are generally depleted (more
133 negative $\delta^{18}\text{O}$ or δD) in summer precipitation at the monsoon region because of continuous
134 upstream distillation processes of vapor starting from the remote oceanic moisture source region.
135 In addition, the deuterium excess in summer precipitation ($\text{d-excess}=\delta\text{D}-8\times\delta^{18}\text{O}$)
136 (Dansgaard,1964) is also low due to limited kinetic evaporation over the oceanic moisture source
137 region under high surface air humidity conditions.

138 After the retreat of the summer monsoon, the Mongolia High (also called Siberia-Mongolia
139 High) starts to strengthen due to gradual cooling of the Eurasia, indicating the switch from the
140 summer monsoon to the winter/non-monsoon season (October to May). In winter, air masses
141 over Nanjing mainly originate from the northwest forced by the Mongolia High (Fig. 2d), and
142 precipitation is generally derived from continental moisture sources and recycling, which tend to
143 enrich heavy isotopes, leading to high isotopic values ($\delta^{18}\text{O}$, δD and d-excess).

144



145

146 Fig. 2. Change in TSV (total spatial variance) as clusters combined (left); and spatial distribution
 147 of vapor trajectories (right) for all precipitation events at Nanjing from September 2011 to
 148 November 2014: (a) and (b) are for the summer monsoon season (June-September); (c) and (d)
 149 are for the non-monsoon season (October to May). The vapor trajectories were simulated by the
 150 Hybrid Single-Particle Lagrangian Integrated Trajectories (HYSPLIT). Vapor trajectories back to
 151 11 d at 1500 m AGL (above ground level) were calculated for the summer monsoon season as
 152 water vapor transport is usually concentrated in the middle and lower troposphere (Bershaw et al.,
 153 2012). The moisture transport paths back to 7d at 500 m AGL were determined for the
 154 non-monsoon season because of higher wind speed and lower condensation height in the

155 non-monsoon season. The total spatial variance (TSV) was used to identify the optimum number
156 of clusters.

157

158 **3 Methods and materials**

159 Using a rain gauge, precipitation samples were collected on days with precipitation greater
160 than 0.1 mm from September 2011 to November 2014 with the exception of January-April 2013.
161 It was carried out at the Station for Observing Regional Processes of the Earth System (SORPES)
162 at Nanjing University (Ding et al., 2013). A narrow mouth container with a diameter of one
163 centimeter was used in order to minimize evaporation. Samples were collected as soon as
164 possible after rainfall events, and were immediately poured into 100 mL polyethylene bottles,
165 which were then sealed and frozen for storage.

166 The $\delta^{18}\text{O}$ and δD of these samples were simultaneously measured using a Picarro L2120-i
167 wavelength scanned-cavity ring down spectroscopy (WS-CRDS) system at the Key Laboratory
168 of Coast and Island Development of the Ministry of Education, School of Geographic and
169 Oceanographic Sciences, Nanjing University, China.

170 The stable isotopic ratio was calculated as:

$$171 \quad \delta = \left[\frac{R_{\text{sample}}}{R_{\text{reference}}} - 1 \right] \times 1000 \text{‰}$$

172 where R is the ratio of the composition of the heavier to lighter isotopes in water ($^{18}\text{O}/^{16}\text{O}$ for
173 $\delta^{18}\text{O}$, or D/H for δD), and the reference is the Vienna Standard Mean Ocean Water standard.
174 Each sample was measured eight times. The maximum peak drift in 24 hours of Picarro L2120-i
175 is less 0.6‰ for $\delta^{18}\text{O}$ and 1.8‰ for δD . In order to reduce the influence of instrument drift,
176 internal water standard samples were inserted among the samples for measurements (one water

177 standard sample for every 7 samples). The first five measurements were discarded in order to
178 eliminate the effect of memory. The average of the last three measurements was calibrated based
179 on the linear regression between the known isotopic values of our three internal water standards
180 and their measured values. The calibrated values of samples were taken as the test results. The
181 analytical uncertainty is less than 0.1‰ for $\delta^{18}\text{O}$ and 0.5‰ for δD . A quadratic error for d-excess
182 is less than 1.0‰, estimated by the uncertainties of $\delta^{18}\text{O}$ and δD .

183 In order to link precipitation stable isotopes with weather conditions, the daily
184 meteorological data were obtained from the China Meteorological Data Sharing Service System,
185 which included precipitation amount, surface air temperature, evaporation and relative humidity
186 at Nanjing during the observation period. Additional data were obtained from National Centers
187 for Environmental Prediction/National Center for Atmospheric Research (NCEP/NCAR)
188 reanalysis data in order to identify changes of moisture source and vapor transport. They include
189 the daily OLR, horizontal wind fields, and specific humidity, provided by the
190 NOAA/ORA/ESRL PSD, Boulder, Colorado, USA, from their Web site at
191 <http://www.esrl.noaa.gov/psd>.

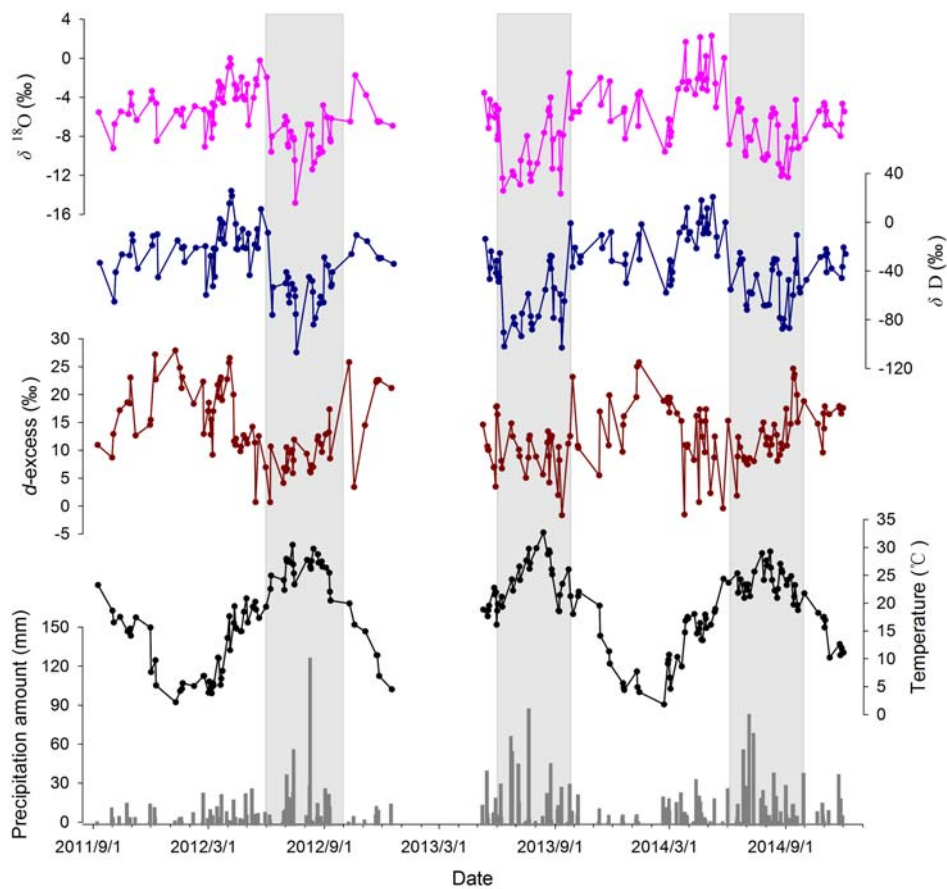
192

193 **4 Results**

194 **4.1 Seasonal variations of stable isotopes in precipitation**

195 Temporal variations of daily precipitation stable isotopes ($\delta^{18}\text{O}$, δD and d-excess),
196 precipitation amount, and surface air temperature in Nanjing during the observation period are
197 presented in Fig. 3. The isotopic data exhibits significant seasonal variations, with low values of
198 the $\delta^{18}\text{O}$, δD and d-excess in the summer monsoon season and high values in the non-monsoon

199 season. The values in the summer monsoon season (the non-monsoon season) range from
 200 -14.8‰ to -1.5‰ (-9.5‰ to 2.3‰) for $\delta^{18}\text{O}$, from -106.0‰ to -0.3‰ (-59.0‰ to 26.2‰) for δD ,
 201 and from -1.4‰ to 24.8‰ (-1.3‰ to 28.1‰) for d-excess. The precipitation-weighted mean
 202 isotopic value in the summer monsoon season (the non-monsoon season) is -9.1‰ (-4.9‰) for
 203 $\delta^{18}\text{O}$, -61.8‰ (-23.4‰) for δD , and 10.9‰ (15.5‰) for d-excess.



204

205 Fig. 3. Temporal variations of daily precipitation $\delta^{18}\text{O}$, δD , d-excess, surface air temperature and
 206 precipitation amount in Nanjing from September 2011 to November 2014. The shaded areas
 207 represent the summer monsoon seasons (June to September). Data is missing from January to
 208 April 2013.

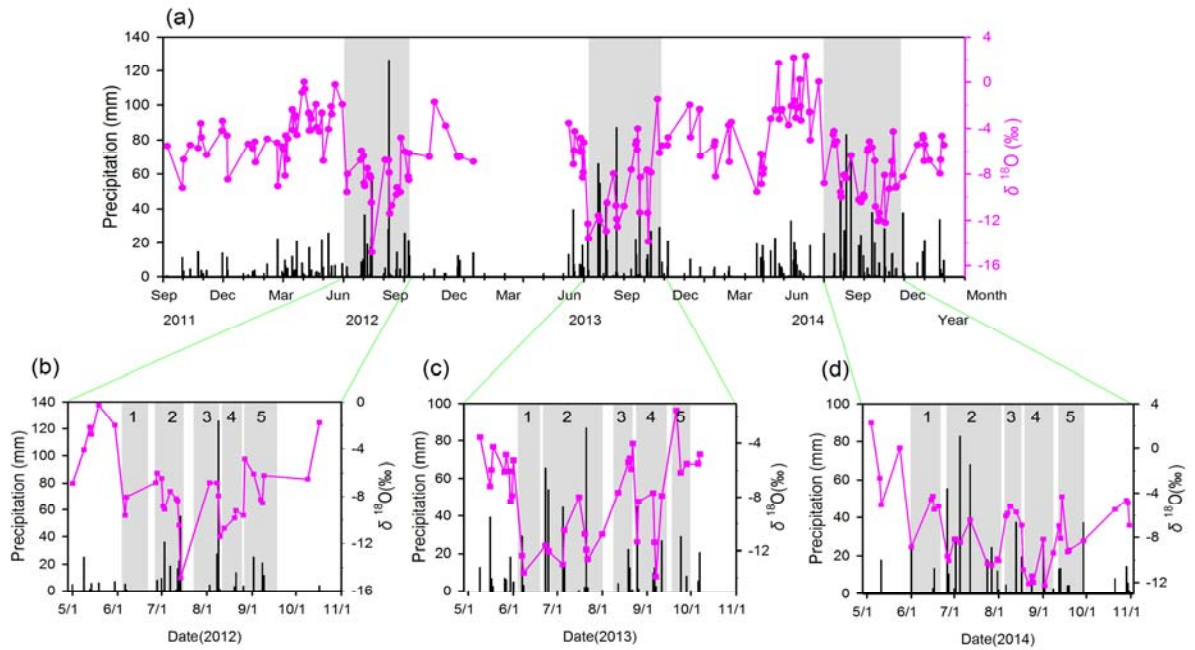
209

210 **4.2 $\delta^{18}\text{O}$ variations in summer precipitation**

211 In 2012, after a sudden decrease on June 6, the precipitation $\delta^{18}\text{O}$ remained low, reaching a
212 minimum (-14.8‰) on July 14. The $\delta^{18}\text{O}$ values increased in early August, and decreased again
213 in late August. In early September, $\delta^{18}\text{O}$ in precipitation became enriched (Fig. 4b). In 2013,
214 precipitation $\delta^{18}\text{O}$ decreased suddenly on June 7, then increased slowly until it peaked (-4.0‰)
215 on August 22. The stable isotope composition was depleted in late August and reached a
216 minimum (-13.8‰) on September 7. In late September, $\delta^{18}\text{O}$ in precipitation was enriched (Fig.
217 4c). In 2014, $\delta^{18}\text{O}$ in precipitation decreased on June 1 and slightly increased afterward until it
218 was depleted again in July. It started to increase in early August. From late August to early
219 September, $\delta^{18}\text{O}$ in precipitation remained depleted, but became enriched since late September
220 (Fig. 4d).

221 We divided the summer into 5 distinct stages (Figure 4), based on the temporal patterns of
222 $\delta^{18}\text{O}$ variations and **official designation of Meiyu period in the study area**. Stage 1 started with
223 the sudden decrease in $\delta^{18}\text{O}$ in early June, which is generally considered an indicator for the
224 onset of the summer monsoon (e.g., Tian et al., 2001; Vuille et al., 2005; Yang et al., 2012). Stage
225 2 covered the Meiyu period. The start dates of Meiyu in 2012–2014 were June 26, June 23, and
226 June 25 respectively, according to the observations made by the Jiangsu Provincial
227 Meteorological Bureau. Stage 3 was characterized by relatively high precipitation $\delta^{18}\text{O}$, whereas
228 in stage 4, $\delta^{18}\text{O}$ remained low. Stage 5 marked the return of $\delta^{18}\text{O}$ values to enriched state. The 5
229 stages were delineated in Figure 4(b)-(d).

230



231

232 Fig. 4. (a) Temporal variation of daily precipitation $\delta^{18}\text{O}$ and precipitation amount from
 233 September 2011 to November 2014 (Data is missing for $\delta^{18}\text{O}$ from January to April 2013). (b) –
 234 (d): Temporal variations in daily precipitation $\delta^{18}\text{O}$ and local precipitation amount from May to
 235 October in 2012 (b), 2013 (c), 2014 (d). The shaded bars represent different stages.

236 In (b) for 2012, stage 1: June 3 - June 20; stage 2: June 27 - July 14; stage 3: July 20 - August 9;
 237 stage 4: August 10 - August 26; and stage 5: August 27 - September 20.

238 In (c) for 2013, stage 1: June 7 - June 20; stage 2: June 23 - August 1; stage 3: August 12 -
 239 August 22; stage 4: August 25 - September 11; and stage 5: September 20 - September 30.

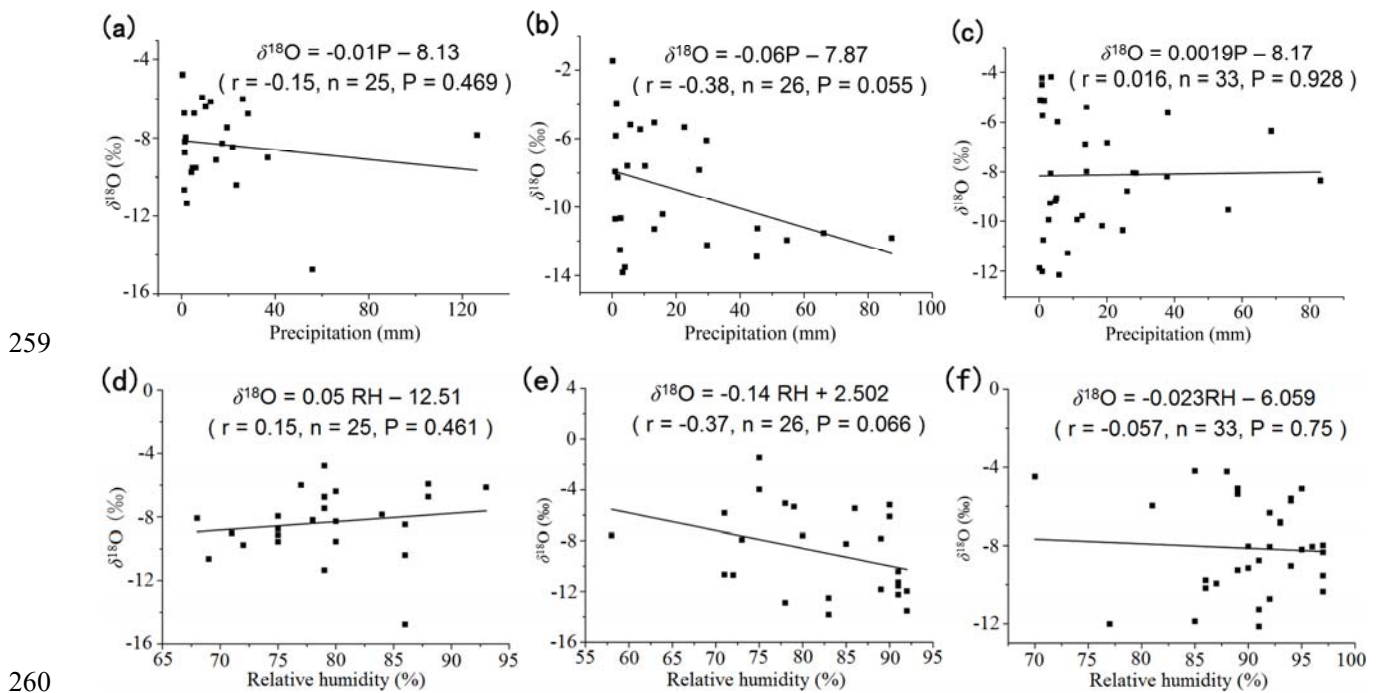
240 In (d) for 2014, stage 1: June 1 - June 20; stage 2: June 26 - August 1; stage 3: August 6 - August
 241 17; stage 4: August 18 - September 8; and stage 5: September 12 - September 30.

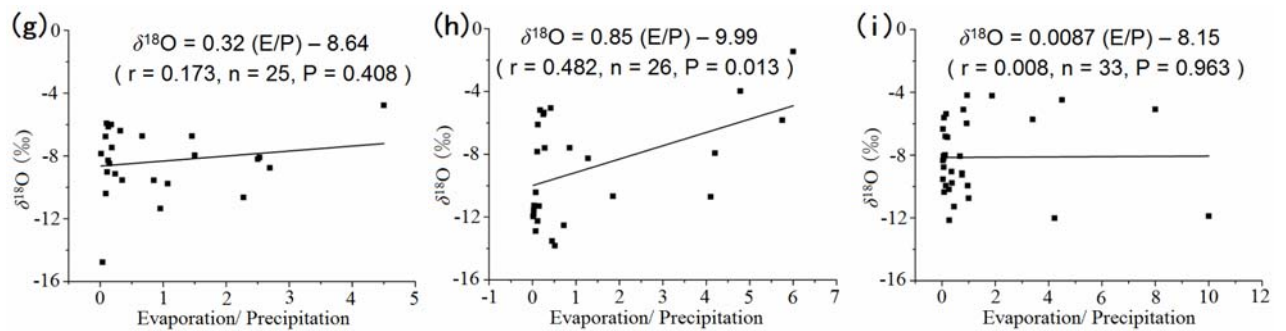
242

243 4.3 The amount effect of $\delta^{18}\text{O}$ in summer precipitation

244 The amount effect refers to the observed negative correlation between precipitation isotopic
 245 composition and precipitation amount (Dansgaard, 1964). The most discussed mechanism for the

246 amount effect is that high precipitation rates increase relative humidity, hence decrease
 247 evaporation. As evaporation serves to enrich heavy isotopes, its reduction leads to more depleted
 248 precipitation isotopic signatures. Moreover, high relative humidity also inhibits re-evaporation of
 249 local surface water (lakes and streams) to feed back into the precipitation. As local surface water
 250 is usually more enriched in heavy isotopes, its diminished input also leads to more depleted
 251 precipitation isotopic composition. Here we investigated if the amount effect could be clearly
 252 observed from our data. We performed separate correlation analyses between precipitation $\delta^{18}\text{O}$
 253 and precipitation amount, relative humidity and the evaporation ratio defined as evaporation
 254 divided by precipitation (E/P) (Fig. 5). There was a weak negative correlation between
 255 precipitation $\delta^{18}\text{O}$ and precipitation amount for 2013 (Fig. 5b). In addition, precipitation $\delta^{18}\text{O}$
 256 became more depleted with increased relative humidity (Fig. 5e) and decreased E/P ratio (Fig. 5h)
 257 for the same year. This seems to suggest that the amount effect was present in the 2013 data.
 258 However, no significant correlation was observed for the 2012 and 2014 data (Fig. 5a, c).





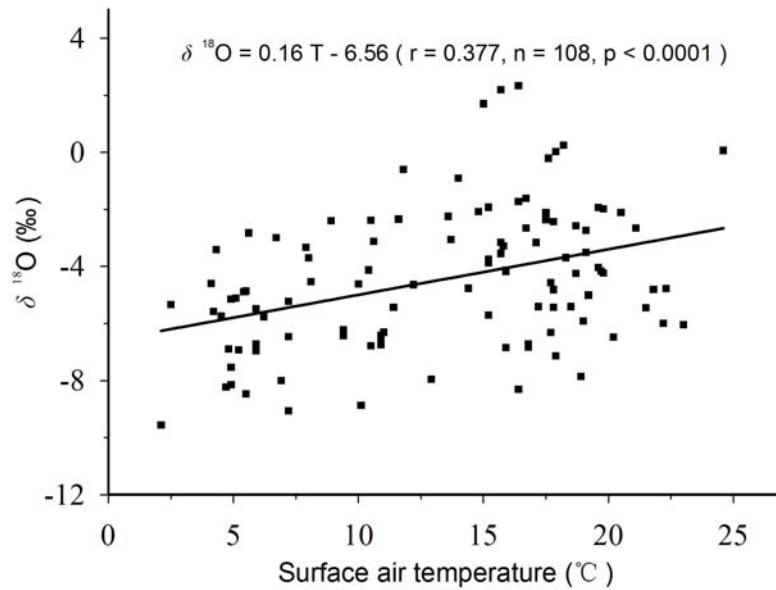
261

262 Fig. 5. This figure shows: (1) correlation between $\delta^{18}\text{O}$ and precipitation amount in Nanjing from
 263 June to September for 2012 (a), 2013 (b) and 2014 (c); (2) correlation between $\delta^{18}\text{O}$ and relative
 264 humidity in Nanjing from June to September for 2012 (d), 2013 (e) and 2014 (f); (3) correlation
 265 between $\delta^{18}\text{O}$ and evaporation/precipitation (E/P) ratio in Nanjing from June to September for
 266 2012 (g), 2013 (h) and 2014 (i). Linear regression lines, correlation coefficient r and p -values are
 267 also shown.

268

269 4.4 The temperature effect of $\delta^{18}\text{O}$ in non-monsoonal precipitation

270 In our study area, the $\delta^{18}\text{O}$ values in non-monsoonal precipitation was primarily influenced
 271 by the temperature effect, even though such effect is often dampened or even reversed in
 272 summer for southeast Asia due to the summer monsoon influence (Araguas-Araguas et al., 1998).
 273 Our data clearly showed a significant positive correlation between the daily precipitation $\delta^{18}\text{O}$
 274 and surface air temperature in the non-monsoon seasons of the observation period, with a linear
 275 T- $\delta^{18}\text{O}$ relationship: $\delta^{18}\text{O} = 0.16 T - 6.56$ (Fig. 6).



276

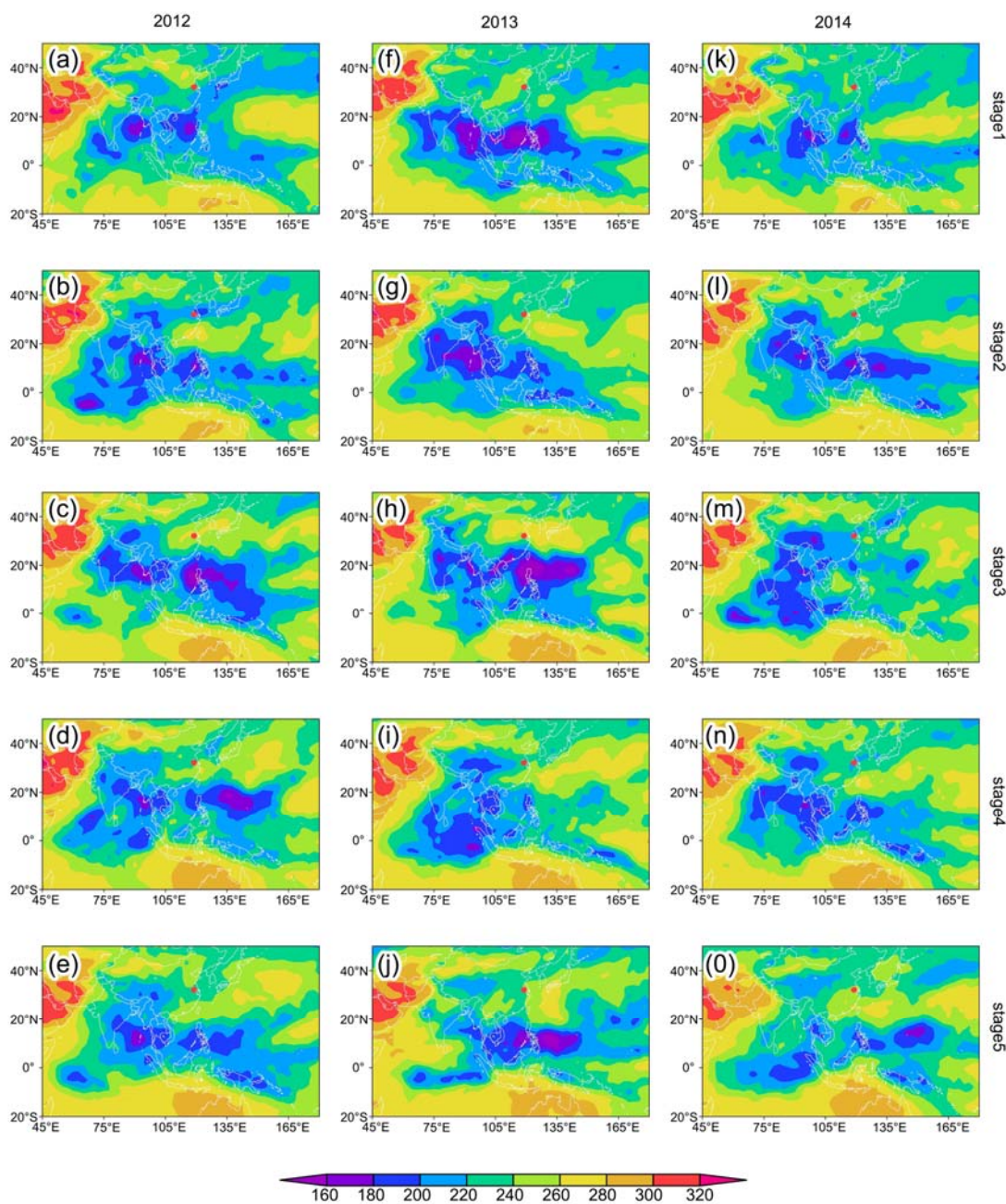
277 Fig. 6. Correlation between daily precipitation $\delta^{18}\text{O}$ and surface air temperature in the
 278 non-monsoon seasons of the observation period in Nanjing. Linear regression line, correlation
 279 coefficient r and p -values are also shown.

280

281 5 Discussion

282 The ITCZ region is an important moisture source for precipitation in general, and for
 283 monsoon precipitation in particular. In fact, the monsoon is often considered a manifestation of
 284 the intraseasonal migration of the ITCZ (Gadgil, 2003). To explore the possible influence of
 285 ITCZ intensity and position on $\delta^{18}\text{O}$ in summer precipitation in Nanjing, a composite analysis of
 286 OLR was performed for each stage (Fig. 7). Low OLR values correspond to cold and high clouds
 287 associated with enhanced convection, and a negative relationship is generally observed between
 288 OLR and convection intensity (Wang et al., 1997). Therefore, a composite analysis of OLR could
 289 help establish the location and intensity of deep convections associated with the ITCZ, which
 290 serve as moisture sources for the monsoon precipitation in Nanjing. It was also necessary to
 291 establish the moisture transport magnitude and pathways for each stage in order to link the

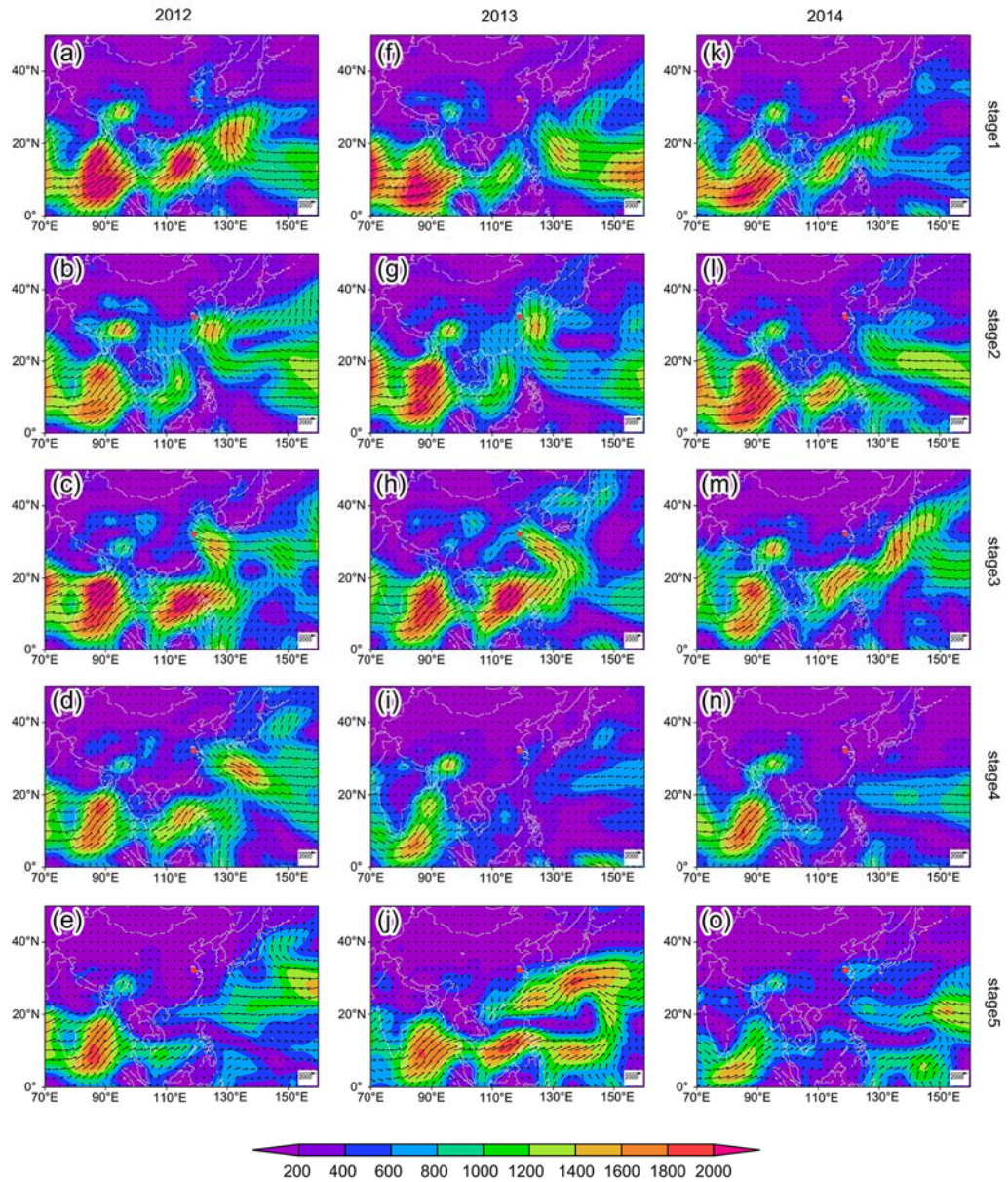
292 source regions with our study area, as both could potentially influence the precipitation $\delta^{18}\text{O}$.
 293 This was achieved by vertically integrating mean water vapor transport for each stage, using the
 294 daily NCEP/NCAR reanalysis data (Fig. 8). Water vapor transport was calculated as the
 295 horizontal wind field (zonal and meridional winds) multiplied by specific humidity, which was
 296 then integrated from surface to 300 hPa level.



297

298 Fig. 7. Composite results for average OLR (W m^{-2}) for stages 1 to 5 in 2012 (a – e), 2013 (f – j)

299 and 2014 (k – o). The convective activity is indicated by low values in OLR. Daily OLR data at
 300 $2.5^\circ \times 2.5^\circ$ resolution were used. The study site of Nanjing is marked by the red dot.
 301



302
 303 Fig. 8. Vertically integrated mean water vapor transport ($\text{g cm}^{-1} \text{s}^{-1}$) for stages 1-5 in 2012 (a – e),
 304 2013 (f – j) and 2014 (k – o). Different colors indicate the magnitude of the moisture flux vector.
 305 The study site of Nanjing is marked by the red dot.

306

307 In stage 1, the abrupt decrease of $\delta^{18}\text{O}$ indicated the onset of the Asian summer monsoon,
308 with strong ITCZ convections in the Bay of Bengal and the South China Sea (Fig. 7a, f, k), and
309 the delivery of moisture from both regions (Fig. 8a, f, k). The isotope fractionation that occurred
310 during the strong convection and the transport process lightened the stable isotopes in water
311 vapor, resulting in the abrupt decrease of $\delta^{18}\text{O}$ in precipitation in Nanjing.

312 In stage 2, the ITCZ intensity and location in 2012 did not change significantly from stage 1
313 (Fig. 7b), and $\delta^{18}\text{O}$ remained low. The extreme negative $\delta^{18}\text{O}$ on July 14 was due to the
314 continuous local rainfall from July 12 to 14, further depleting $\delta^{18}\text{O}$ in precipitation. In 2013, the
315 ITCZ intensity did not change much in the Bay of Bengal, but decreased significantly in the
316 South China Sea and the low-latitude western Pacific Ocean (Fig. 7g). Weak convection reduced
317 the rainout effect, and hence increased $\delta^{18}\text{O}$ in precipitation. In 2014 the ITCZ intensity
318 increased in the South China Sea and the low-latitude western Pacific Ocean, but it did not
319 change significantly in the Bay of Bengal (Fig. 7l). At this stage, as the meridional water vapor
320 transport to the north from the South China Sea increased (Fig. 8b, g, l), changes in convective
321 activity in the South China Sea had a stronger influence on $\delta^{18}\text{O}$ in study area precipitation.
322 Strong convection in the South China Sea enhanced rainout effect, resulting in depleted $\delta^{18}\text{O}$ in
323 precipitation in Nanjing.

324 In stage 3, the ITCZ intensity decreased in the Bay of Bengal in both 2012 and 2013, but
325 increased in the South China Sea and the low-latitude western Pacific Ocean. The center of
326 strong convection propagated northward (Fig. 7c, h). Water vapor mainly originated from the
327 South China Sea and the low-latitude western Pacific Ocean (Fig. 8c, h) for this stage. The
328 relatively shorter transport distance resulted in higher $\delta^{18}\text{O}$ values in precipitation. In 2014, the

329 ITCZ intensity was relatively low in the South China Sea and the low-latitude western Pacific
330 Ocean (Fig. 7m). The water vapor came mainly from the adjacent seas (Fig. 8m). As a result, the
331 relatively weak convection in the area and short transport distance enriched $\delta^{18}\text{O}$ in precipitation
332 in Nanjing.

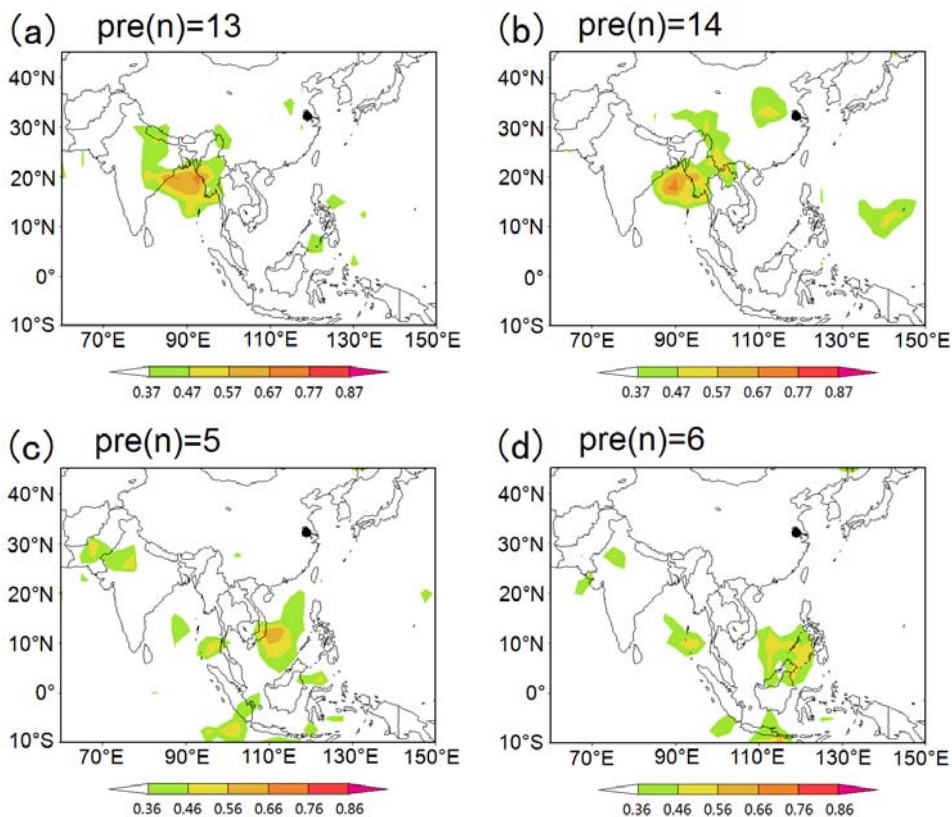
333 Stage 4 covered the late monsoon season. In 2012, in addition to increased convection
334 strength in the west Pacific Ocean, the strong convective center also moved eastward (Fig. 7d),
335 increasing the water transport distance to Nanjing. Both of these changes acted to deplete $\delta^{18}\text{O}$ in
336 precipitation. Moreover, the moisture transport suggested that vapor from the Bay of Bengal was
337 also transported to Nanjing (Fig. 8d). The strong convection in the Bay of Bengal and its long
338 distance from the study site contributed to further deplete $\delta^{18}\text{O}$ in precipitation. In 2013 and 2014,
339 the ITCZ intensity in the South China Sea and the western Pacific was relatively weak (Fig. 7i,
340 n). However, both the moisture transport from the Bay of Bengal (Fig. 8i, n) and the convective
341 activity in the Bay of Bengal was strong (Fig. 7i, n). In addition, the strong convective center in
342 the Bay of Bengal moves southward in stage 4 of 2013 (Fig. 7i) resulting in longer distance
343 **transport to** Nanjing. The combination of these factors depleted the isotopic composition of
344 precipitation in this stage for both 2013 and 2014. **This is consistent with** the time series of $\delta^{18}\text{O}$
345 in precipitation showed a clear trend of decreasing $\delta^{18}\text{O}$ -values during the late monsoon period,
346 while rainfall peaked earlier in the season. The depleted $\delta^{18}\text{O}$ values in late monsoon season were
347 also observed in the other monsoon areas. Pang et al. (2006) suggested that the low $\delta^{18}\text{O}$ values
348 were caused by the recycling of monsoon precipitation in late monsoon season. Breitenbach et al.
349 (2010), on the other hand, argued that the Bay of Bengal freshwater plume, consisted of
350 isotopically depleted rain water and snow melt water, diluted the Bay of Bengal surface water

351 $\delta^{18}\text{O}$ pool in late monsoon season. This contributed to the depleted $\delta^{18}\text{O}$ in precipitation. Our
352 results suggest that the depleted precipitation $\delta^{18}\text{O}$ in the late monsoon season could result from
353 the combination of increased convective activities and transport distance due to the retreat of the
354 ITCZ southward in the Bay of Bengal.

355 In stage 5, the Asian summer monsoon retreated and water vapor from the inland areas with
356 a high stable isotopic composition was transported to Nanjing (Fig. 8e, j, o), enriching the $\delta^{18}\text{O}$
357 in precipitation. It is worth noting that the ITCZ intensity in the South China Sea and the
358 low-latitude western Pacific Ocean strengthened in stage 5 of 2013 because of the super Typhoon
359 Usagi (Fig. 7j). However, Nanjing was not affected due to its location at the edge of the Typhoon.
360 At the time, the moisture in Nanjing came mainly from the northern inland areas and the adjacent
361 seas in the northeast (Fig. 8e, j, o). Therefore, the stable isotopic composition of precipitation
362 remained enriched.

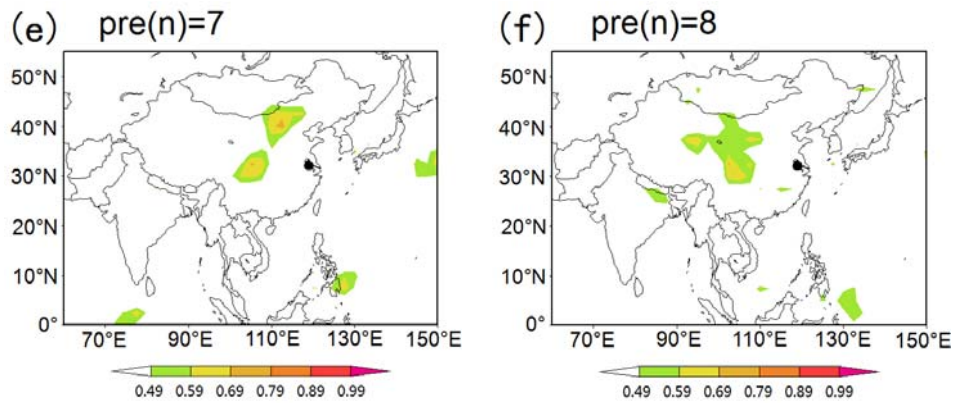
363 The above observations seem to suggest that summer precipitation $\delta^{18}\text{O}$ in Nanjing were
364 closely related to changes in moisture source and convective activity within moisture source
365 regions. In order to further explore this relationship quantitatively, we performed a time-lagged
366 spatial correlation analysis between precipitation $\delta^{18}\text{O}$ in Nanjing and the daily OLR time series.
367 Several patterns emerged from this analysis. For stage 1 and 4, the strongest positive correlation
368 between $\delta^{18}\text{O}$ and OLR in the Bay of Bengal occurred at 13 and 14 days before the rainfall (Fig.
369 9a, b). This supports the conclusion of previous studies that convective processes could have
370 integrated impacts on water vapor over several days preceding precipitation events (Tremoy et
371 al., 2012; Gao et al., 2013). For stage 2, our analysis showed the strongest positive correlation
372 between $\delta^{18}\text{O}$ and the OLR in the South China Sea at 5 and 6 days preceding the rainfall (Fig. 9c,

373 d). This **supports** the significant influence of convective intensity in the South China Sea on $\delta^{18}\text{O}$
 374 in precipitation in Nanjing at stage 2. As this stage covered the Meiyu period, this result is
 375 largely in agreement with previous studies, which indicate that moisture for Meiyu precipitation
 376 mainly comes from the South China Sea (Simmonds et al., 1999; Ding et al., 2007). For stage 5,
 377 the strongest positive correlation between daily $\delta^{18}\text{O}$ in precipitation and OLR in the inland areas
 378 to the north and west was observed at 7 and 8 days before the rainfall (Fig. 9e, f), suggesting that
 379 inland vapor contributed to $\delta^{18}\text{O}$ in precipitation after the monsoon withdrew. However, no
 380 significant correlation between $\delta^{18}\text{O}$ and OLR was found for stage 3. This could partially
 381 attributed to the shift of ITCZ location northward and eastward in 2012 and 2013 (Fig. 7c, h),
 382 reducing the vapor transport distance (Fig. 8c, h). This could have played a more important role
 383 in determining the $\delta^{18}\text{O}$ values in precipitation in Nanjing than convective intensity.



384

385



386

387 Fig. 9. Spatial correlation between daily $\delta^{18}\text{O}$ in precipitation and OLR at n days prior to the
 388 rainfall date: Spatial correlation between $\delta^{18}\text{O}$ in precipitation and OLR at 13 days (a) and 14
 389 days (b) prior to the rainfall date for stages 1 and 4; Spatial correlation between $\delta^{18}\text{O}$ in
 390 precipitation and OLR at 5 days (c) and 6 days (d) prior to the rainfall date for stage 2; Spatial
 391 correlation between $\delta^{18}\text{O}$ in precipitation and OLR at 7 days (e) and 8 days (f) prior to the
 392 rainfall date for stage 5. For all maps, only areas with correlations significant at 0.05 level are
 393 shown. The study site Nanjing is marked with a black dot.

394

395 Our results suggest that **changes in moisture source and** the upstream convective activity over
 396 the tropical regions of the Bay of Bengal, the South China Sea and the western Pacific have an
 397 important impact on the daily isotopic composition of summer precipitation in Nanjing. Strong
 398 distillation processes during intense convective activity would increase the rainout of heavy
 399 isotopes upstream, hence deplete the isotopic composition in precipitation downstream, and vice
 400 versa. Therefore, the daily isotopic composition in summer precipitation downstream of the
 401 moisture sources in the tropics could be determined mainly by changes of the isotopic
 402 composition of atmospheric vapor in the upstream source region rather than the precipitation
 403 amount on site. **It should be noted that although such effects as the changes in moisture source**

404 and the upstream rainout on stable isotopes in precipitation could clearly be observed on the
405 intra-seasonal time scale, as discussed above, they may not be significant on inter-annual to
406 decadal time scales because of insufficient changes in moisture source and the upstream rainout
407 when averaged at these time scales. Nevertheless, these effects could be important on longer
408 time scales (centennial to orbital time scales), such as the glacial-interglacial time scale, when
409 moisture source locations and the upstream rainout processes could vary remarkably. Pausata et
410 al. (2011) used a climate model with an embedded oxygen-isotope model to simulate a Heinrich
411 event and found that the variations of stalagmite $\delta^{18}\text{O}$ values in southern China mainly reflected
412 $\delta^{18}\text{O}$ changes in the source vapor from the Indian Ocean rather than local precipitation amount.
413 Liu et al. (2015) also indicated that the stalagmite $\delta^{18}\text{O}$ records during the Holocene from the
414 East Asian summer monsoon region are essentially a signal of the isotopic composition of
415 precipitation, which is largely determined by the upstream depletion mechanism over the Indian
416 Ocean and the Indian monsoon region.

417 Although changes in moisture source and upstream rainout effect seem to be the main
418 controlling factors for the intra-seasonal isotopic variations of precipitation at Nanjing during
419 summer monsoon season, a correlation between the $\delta^{18}\text{O}$ and precipitation amount did exist in
420 the summer of 2013 (Fig. 5b). To examine this further, we downloaded data from the Global
421 Network for Isotopes in Precipitation (GNIP) (<http://isohis.iaea.org/gnip.asp>) for Nanjing
422 covering the summers of 1987-1992, and found a weak but statistically significant negative
423 correlation between the monthly isotopic composition ($\delta^{18}\text{O}$ or δD) and precipitation amount.
424 This seems to suggest that the amount effect could still play an important role, particularly at the
425 time scales when precipitation varied greatly, such as the glacial-interglacial climate cycles. In

426 addition, there is likely considerable amount of local evapotranspiration in the Asian monsoon
427 region because of high vegetation cover under humid monsoon climate conditions. How local
428 evapotranspiration affects the summer precipitation $\delta^{18}\text{O}$ is still unclear and requires further
429 study.

430 The linear slope between the daily surface air temperature and $\delta^{18}\text{O}$ in non-monsoonal
431 precipitation in Nanjing is $0.16\text{‰}/^{\circ}\text{C}$ based on our observations. This is largely consistent with
432 the slope ($0.20\text{‰}/^{\circ}\text{C}$) calculated from the GNIP Nanjing station data. This confirms the
433 temperature effect of stable isotopes in the non-monsoon season. By comparison, the correlation
434 between surface air temperature and non-monsoonal precipitation $\delta^{18}\text{O}$ of Nanjing is weaker than
435 those observed in high latitudes. This may be caused by the switch of moisture source from the
436 nearby offshore seas to the remote inland regions of Eurasia (Fig. 2d). In addition, the relatively
437 dry climate condition in the non-monsoon season could increase the potential re-evaporation of
438 precipitation, and affect the isotopic composition of precipitation during its falling. This could
439 also contribute to the weak temperature effect on stable isotopes. **Regardless**, the considerable
440 precipitation amount in the non-monsoon season highlights the importance of the temperature
441 effect for interpretation of stable isotope records in speleothems from the monsoon region. Some
442 studies demonstrated that winter temperature in East China was dominated by the East Asian
443 winter monsoon associated with the Mongolia High (Guo, 1994; Liu et al., 2011).

444 Based on the above analysis, the isotopic composition of precipitation preserved in
445 speleothems in the East Asian monsoon region is likely controlled by both the East Asian
446 summer and winter monsoon processes. Indeed, Clemens et al. (2010) suggested that the timing
447 of light $\delta^{18}\text{O}$ peaks in speleothems from southeast China on the orbital time scale were controlled

448 by both strong summer monsoons and winter temperature changes. Other studies suggest that the
449 oxygen isotope records in Chinese speleothems indicate changes in the ratio of summer to winter
450 precipitation (Wang et al., 2001; Yuan et al., 2004; Dykoski et al., 2005; Kelly et al., 2006; Wang
451 et al., 2008; Zhang et al., 2008; Cheng et al., 2009). However, this inference is not backed up by
452 any physical mechanisms, as various factors affecting stable isotopes of precipitation were not
453 considered. Indeed, no correlation was found between the annual mean weighted-precipitation
454 $\delta^{18}\text{O}$ and the ratio of summer to winter precipitation in the combined data from our observation
455 (2012-2014) and the GNIP data (1987-1992). Years with more than two months of missing data
456 were excluded from the analysis.

457 In summary, when interpreting the oxygen isotopic records in speleothems in the Asian
458 monsoon region at longer time scales such as the glacial-interglacial climate cycles, both the
459 upstream rainout effect on stable isotopes related to changes in the Asian summer monsoon and
460 the temperature effect associated with winter monsoon should be considered. Both effects could
461 be evaluated by present-day observation and historical simulations of water stable isotopes in the
462 general circulation models (Risi et al., 2010; Werner et al., 2011).

463

464 **6 Conclusions**

465 We found that the intra-seasonal variations of $\delta^{18}\text{O}$ of precipitation in Nanjing during
466 summer were closely related to changes in the location and convection intensity in moisture
467 sources. At the onset of the summer monsoon (stage 1), vapor to our study site was mainly
468 transported from the Bay of Bengal, where the strong convection in the source area and its
469 relatively long distance from our study area acted to decrease $\delta^{18}\text{O}$ in precipitation in Nanjing.

470 During the Meiyu period (stage 2), water vapor came mainly from the South China Sea, and
471 changes in ITCZ intensity in the South China Sea led to the variability of $\delta^{18}\text{O}$ in precipitation in
472 Nanjing. The northward propagation of the ITCZ during the mid-monsoon season (stage 3)
473 reduced the vapor transport distance, resulting in relatively enriched $\delta^{18}\text{O}$. During the late
474 monsoon period (stage 4), the ITCZ retreated to the Bay of Bengal. The strong convection and
475 relatively long-distance vapor transport again led to depleted $\delta^{18}\text{O}$ values in precipitation in
476 Nanjing. Finally, when the monsoon withdrew (stage 5), vapor from the north and west inland
477 areas contributed to the enriched $\delta^{18}\text{O}$. The results indicate that the changes in the ITCZ location
478 and intensity are major factors affecting the stable isotopes in summer precipitation in Nanjing.
479 Therefore, the stable isotopes in precipitation could signal a shift of moisture source regions and
480 ITCZ over the course of monsoon season. Our analyses suggest that changes in moisture sources
481 and upstream rainout effect should be taken into account when interpreting the stable isotopic
482 composition of speleothems in the Asian monsoon region. However, the temperature effect of
483 stable isotopes in precipitation during the non-monsoon season is also important because almost
484 half of the annual precipitation occurs in the non-monsoon season.

485

486 **Acknowledgments**

487 We thank the NOAA Air Resources Laboratory (ARL) for providing the HYSPLIT model
488 used in this study. This work was supported by the Natural Science Foundation of China
489 (41330526, 41171052 and 41321062), **the Natural Science Foundation of Jiangsu Province**
490 **(BK20151387)**, and the Priority Academic Program Development of Jiangsu Higher Education
491 Institutions (PAPD).

492 **References:**

- 493 Ananthakrishnan, R., Pathan, J. M., and Aralikatti, S. S.: On the northward advance of the ITCZ
494 and the onset of the southwest monsoon rains over the southeast Bay of Bengal, *Int. J.*
495 *Climatol.*, 1,153-165, 1981.
- 496 Araguás-Araguás, L., Froehlich, K., and Rozanski, K.: Stable isotope composition of
497 precipitation over southeast Asia, *J. Geophys. Res.*, 103(D22), 28721-28742, 1998.
- 498 Bershaw, J., Penny, S. M., and Garziona, C. N.: Stable isotopes of modern water across the
499 Himalaya and eastern Tibetan Plateau: implications for estimates of paleoelevation and
500 paleoclimate, *J. Geophys. Res.*, 117: D02110, doi:10.1029/2011JD016132, 2012.
- 501 Breitenbach, S. F. M., Adkins, J. F., Meyer, H., Marwan, N., Kumar, K. K., and Haug, G. H.:
502 Strong influence of water vapor source dynamics on stable isotopes in precipitation observed
503 in Southern Meghalaya, NE India, *Earth. Planet. Sci. Lett.*, 292, 212-220, 2010.
- 504 Cai, Y. J., Tan, L. C., Cheng, H., An, Z. S. Edwards, R. L., Kelly, M. J., Kong, X. G., and Wang,
505 X. F.: The variation of summer monsoon precipitation in central China since the last
506 deglaciation, *Earth Planet. Sci. Lett.*, 291, 21-31, 2010.
- 507 Cheng, H., Edwards, R. L., Broecker, W. S., Denton, G. H., Kong, X. G., Wang, Y. J., Zhang, R.,
508 and Wang, X. F.: Ice Age Terminations, *Science*, 326, 248-252, 2009.
- 509 Clemens, S. C., Prell, W. L., and Sun, Y.: Orbital-scale timing and mechanisms driving Late
510 Pleistocene Indo-Asian summer monsoons: Reinterpreting cave speleothem $\delta^{18}\text{O}$,
511 *Paleoceanography*, 25, PA4207, doi:10.1029/2010PA001926, 2010.
- 512 Conroy, J. L., Cobb, K. M., and Noone, D.: Comparison of precipitation isotope variability
513 across the tropical Pacific in observations and SWING2 model simulations, *J. Geophys. Res.*,

514 118, 5867-5892, 2013.

515 Cruz, F. W., Burns, S. J., Karmann, I., Sharp, W. D., Vuille, M., Cardoso, A. O., Ferrari, J. A.,
516 Dias, P. L. S., and Viana, O. Jr.: Insolation-driven changes in atmospheric circulation over the
517 past 116000 years in subtropical Brazil, *Nature*, 434, 63-66, 2005.

518 Cruz, F. W., Vuille, M., Burns, S. J., Wang, X. F., Cheng, H., Werner, M., Edwards, R. L.,
519 Karmann, Ivo., Auler, A. S., and Nguyen, H.: Orbitally driven east-west antiphasing of South
520 American precipitation, *Nature Geoscience*, 2, 210-214, 2009.

521 Dansgaard, W.: Stable isotopes in precipitation, *Tellus*, 16, 436-468, 1964.

522 Dayem, K. E., Molnar, P., Battisti, D. S., and Roe, G. H.: Lessons learned from oxygen isotopes in
523 modern precipitation applied to interpretation of speleothem records of paleoclimate from
524 eastern Asia, *Earth Planet. Sci. Lett.*, 295, 219-230, 2010.

525 Ding, A. J., Fu, C. B., Yang, X. Q., Sun, J. N., Zheng, L. F., Xie, Y. N., Herrmann, E., Nie, W.,
526 Petäjä, T., Kerminen, V.-M., and Kulmala, M.: Ozone and fine particle in the western Yangtze
527 River Delta: an overview of 1 yr data at the SORPES station, *Atmos. Chem. Phys.*, 13,
528 5813-5830, 2013.

529 Ding, Y. H., Liu, J. J., Sun, Y., Liu, Y. J., He, J. H., and Song, Y. F.: A Study of the
530 Synoptic-Climatology of the Meiyu System in East Asia, *Chinese Journal of Atmospheric
531 Sciences (in Chinese)*, 31, 1082-1100, 2007.

532 Ding, Y. H.: The variability of the Asian summer monsoon, *J. Meteor. Soc. Japan*, 85B, 29, 2007.

533 Dykoski, C. A., Edwards, R. L., Cheng, H., Yuan, D. X., Cai, Y. J., Zhang, M. L., Lin, Y. S.,
534 Qing, J. M., An, Z. S., and Revenaugh, J.: A high-resolution, absolute-dated Holocene and
535 deglacial Asian monsoon record from Dongge Cave, China, *Earth Planet. Sci. Lett.*, 233,

536 71-86, 2005.

537 Gadgil, S.: The Indian monsoon and its variability, *Annu. Rev. Earth Planet. Sci.*, 31, 429-467,
538 2003.

539 Gao, J., Delmotte, V. M., Risi, C., He, Y., and Yao, T. D.: What controls precipitation $\delta^{18}\text{O}$ in the
540 southern Tibetan Plateau at seasonal and intra-seasonal scales? A case study at Lhasa and
541 Nyalam, *Tellus*, 65: 1-14, 2013.

542 Gu, G. J., and Zhang, C. D.: Cloud components of the Intertropical Convergence Zone, *J.*
543 *Geophys. Res.*, 107(D21), 4565, doi:10.1029/2002JD002089, 2002.

544 Guo, Q.: Relationship between the variations of East Asian winter monsoon and temperature
545 anomalies in China, *Quarterly Journal of Applied Meteorology*, 5(2), 218-225, 1994 (in
546 Chinese with English abstract).

547 He, Y., Risi, C., Gao, J., Masson-Delmotte, V., Yao, T., Lai, C., Ding, Y., Worden, J., Frankenberg,
548 C., Chepfer, H., and Cesana, G.: Impact of atmospheric convection on south Tibet summer
549 precipitation isotopologue composition using a combination of in situ measurements, satellite
550 data, and atmospheric general circulation modeling, *J. Geophys. Res. Atmos.*, 120, 3852-3871,
551 doi:10.1002/2014JD022180, 2015.

552 Hu, C. Y., Henderson, G. M., Huang, J. H., Xie, S. C., Sun, Y., and Johnson, K. R.: Quantification
553 of Holocene Asian monsoon rainfall from spatially separated cave records, *Earth Planet. Sci.*
554 *Lett.*, 266, 221-232, 2008.

555 Kelly, M. J., Edwards, R. L., Cheng, H., Yuan, D. X., Cai, Y. J., Zhang, M. L., Lin, Y. S., and An,
556 Z. S.: High resolution characterization of the Asian Monsoon between 146,000 and 99,000
557 years B.P. from Dongge Cave, China and global correlation of events surrounding Termination

558 II, *Palaeogeogr. Palaeoclimatol. Palaeoecol.*, 236, 20-38, 2006.

559 Kurita, N., Ichiyanagi, K., Matsumoto, J., Yamanaka, M. D., and Ohata, T.: The relationship
560 between the isotopic content of precipitation and the precipitation amount in tropical regions. *J.*
561 *Geochem. Explor.*, 102, 113-122. 2009.

562 Kurita, N.: Origin of Arctic water vapor during the ice-growing season, *Geophys. Res. Lett.*, 38,
563 L02709, doi:10.1029/2010GL046064, 2011.

564 Kurita, N.: Water isotopic variability in response to mesoscale convective system over the
565 tropical ocean, *J. Geophys. Res.*, 118, 10376-10390, 2013.

566 Lau, K. M. and Yang, S.: Climatology and interannual variability of the Southeast Asian summer
567 monsoon, *Adv. Atmos. Sci.*, 14, 141-162, 1997.

568 Lau, K. M., Kim, and Yang, S.: Dynamical and boundary forcing characteristics of regional
569 components of the Asian summer monsoon, *J. Climate.*, 13, 2461-2482, 2000.

570 Lawrence, J. R. and Gedzelman, S. D.: Low stable isotope ratios of tropical cyclone rains,
571 *Geophys. Res. Lett.*, 23, 527-530, 1996.

572 Lawrence, J. R., Gedzelman, S. D., Dexheimer, D., Cho, H. K., Carrie, G. D., Gasparini, R.,
573 Anderson, C. R., Bowman, K. P., and Biggerstaff, M. I.: Stable isotopic composition of water
574 vapor in the tropics, *J. Geophys. Res.*, 109, D06115, doi:10.1029/2003JD004046, 2004.

575 Lekshmy, P. R., Midhum, M., Ramesh, R., and Jani, R. A.: ^{18}O depletion in monsoon rain relates
576 to large scale organized convection rather than the amount of rainfall, *Scientific Reports*, 4,
577 5661, doi:10.1038/srep05661, 2014

578 Liu, J., Chen, J., Zhang, X., Li, Y., Rao, Z., and Chen, F.: Holocene East Asian summer monsoon
579 records in northern China and their inconsistency with Chinese stalagmite $\delta^{18}\text{O}$ records,

580 Earth-Science Reviews, 148, 194-208, 2015.

581 Liu, Q., Wang, P., Xu, X., Zhi, H., and Sun, X.: A group of circulation indices of Mongolia High
582 and analysis of its relationship with simultaneous anomaly in the climate of China, Journal of
583 Tropical Meteorology, 27(6), 889-898, 2011 (in Chinese with English abstract).

584 Moerman, J. W., Cobb, K. M., Adkins, J. F., Sodemann, H., Clark, B., and Tuen, A. A.: Diurnal
585 to interannual rainfall variations in northern Borneo driven by regional hydrology, Earth.
586 Planet. Sci. Lett., 369, 108-119, 2013.

587 Oh, T. H., Kwon, W. T., and Ryoo, S. B.: Review of the researches on Changma and future
588 observational study (KORMEX), Adv. Atmos. Sci., 14, 207-222, 1997.

589 Pang, H. X., He, Y. Q., Lu, A. G., Zhao, J. D., Ning, B. Y., Yuan, L. L., and Song, B.:
590 Synoptic-scale variation of $\delta^{18}\text{O}$ in summer monsoon rainfall at Lijiang, China, Chin. Sci.
591 Bull., 51, 2897-2904, 2006.

592 Pang, H., Hou, S., Kaspari, S., and Mayewski, P. A.: Influence of regional precipitation patterns
593 on stable isotopes in ice cores from the central Himalayas, The Cryosphere, 8, 289-301, 2014.

594 Partin, J. W., Cobb, K. M., Adkins, J. F., Clark, B., and Fernandez, D. P.: Millennial-scale trends
595 in west Pacific warm pool hydrology since the Last Glacial Maximum, Nature, 449, 452-455,
596 2007.

597 Paulsen, D. E., Li, H. C., and Ku, T. L.: Climate variability in central China over the last 1270
598 years revealed by high-resolution stalagmite records, Quaten. Sci. Rev., 22, 691-701, 2003.

599 Pausata, F. S., Battisti, D. S., Nisancioglu, K. H., Bitz, C. M.: Chinese stalagmite $\delta^{18}\text{O}$ controlled
600 by changes in the Indian monsoon during a simulated Heinrich event, Nat. Geosci. 4, 474-480,
601 2011.

602 Peng, T. R., Wang, C. H., Huang, C. C., Fei, L. Y., Chen, C. T. A., and Hwong, J. L.: Stable
603 isotopic characteristic of Taiwan's precipitation: A case study of western Pacific monsoon
604 region, *Earth Planet. Sci. Lett.*, 289, 357-366, 2010.

605 Qian, W. H. and Lee, D. K.: Seasonal march of Asian summer monsoon, *Int. J. Climatol.*, 20,
606 1371-1381, 2000.

607 Risi, C., Bony, S., Vimeux, F., and Jouzel, J.: Water-stable isotopes in the LMDZ4 general
608 circulation model: Model evaluation for present-day and past climates and applications to
609 climatic interpretations of tropical isotopic records, *J. Geophys. Res.*, 115, D12118,
610 doi:10.1029/2009JD013255, 2010.

611 Saito, N.: Quasi-stationary waves in mid-latitudes and Baiu in Japan, *J. Meteor. Soc. Japan*, 63,
612 983-995, 1995.

613 Sano, M., Xu, C. X., and Nakatsuka, T.: A 300-year Vietnam hydroclimate and ENSO variability
614 record reconstructed from tree ring $\delta^{18}\text{O}$, *J. Geophys. Res.*, 117, D12115,
615 doi:10.1029/2012JD017749, 2012.

616 Simmonds, I., Bi, D., and Hope, P.: Atmospheric water vapor flux and its association with
617 rainfall over China in summer, *J. Climate.*, 12, 1353-1367, 1999

618 Soderberg, K., Good, S. P., O'Connor, M., Wang, L., Ryan, K., and Caylor, K. K.: Using
619 atmospheric trajectories to model the isotopic composition of rainfall in central Kenya,
620 *Ecosphere*, 4(3): 1-18, 2013.

621 Tan, L. C., Cai, Y. J., Cheng, H., An, Z.S., and Edwards, R. L.: Summer monsoon precipitation
622 variations in central China over the past 750 years derived from a high-resolution
623 absolute-dated stalagmite. *Palaeogeogr. Palaeoclimatol. Palaeoecol.*, 280, 432-439, 2009.

624 Tian, L., Masson-Delmotte, V., Stievenard, M., Yao, T., and Jouzel, J.: Tibetan Plateau summer
625 monsoon northward extent revealed by measurements of water stable isotopes, *J. Geophys.*
626 *Res.*, 106, D22, 28081-28088, 2001.

627 Tierney, J. E., Russell, J. M., Huang, Y. S., Sinninghe Damsté, J. S., Hopmans, E. C., and Cohen,
628 A. S.: Northern hemisphere controls on tropical southeast Africa climate during the past 60000
629 years, *Science*, 322, 252-255, 2008.

630 Tremoy, G., Vimeux, F., Mayaki, S., Souley, I., Cattani, O., Risi, C., Favreau, G., and Oi, M.: A
631 1-year long $\delta^{18}\text{O}$ record of water vapor in Niamey (Niger) reveals insightful atmospheric
632 processes at different timescales, *Geophys. Res. Lett.*, 39, L08805,
633 doi:10.1029/2012GL051298, 2012.

634 Vimeux, F., Tremoy, G., Risi, C., and Gallaire, R.: A strong control of the South American
635 SeeSaw on the intra-seasonal variability of the isotopic composition of precipitation in the
636 Bolivian Andes, *Earth. Planet. Sci. Lett.*, 307, 47-58, 2011.

637 Vuille, M., Werner, M., Bradley, R. S., and Keimig, F.: Stable isotopes in precipitation in the
638 Asian monsoon region, *J. Geophys. Res.*, 110, D23108, doi:10.1029/2005JD006022, 2005.

639 Vuille, M., Werner, M., Bradley, R. S., and Keimig, F.: Stable isotopes in precipitation in the
640 Asian monsoon region, *J. Geophys. Res.*, 110, D23108, doi: 10.1029/2005JD006022, 2005.

641 Wang, B. and Lin, H.: Rainy season of the Asian-Pacific summer monsoon, *J. Climate*, 15,
642 386-398, 2002.

643 Wang, B. and Xu, X. H.: Northern Hemisphere summer monsoon singularities and climatological
644 intraseasonal oscillation, *J. Climate*, 10, 1171-1185, 1997.

645 Wang, Y. J., Cheng, H., Edwards, R. L., An, Z. S., Wu, J. Y., Chen, C. C., and Dorale, J. A.: A

646 high-resolution absolute-dated Late Pleistocene Monsoon record from Hulu Cave, China,
647 Science, 294, 2345-2348, 2001.

648 Wang, Y. J., Cheng, H., Edwards, R. L., Kong, X. G., Shao, X. H., Chen, S. T., Wu, J. Y., Jiang, X.
649 Y., Wang, X. F., and An, Z. S.: Millennial-and orbital-scale changes in the East Asian
650 Monsoon over the past 224,000 years, Nature, 451, 1090-1093, 2008.

651 Werner, M., Langebroek, P. M., Carlsen, T., Herold, M., and Lohmann, G.: Stable water isotopes
652 in the ECHAM5 general circulation model: Toward high-resolution isotope modeling on a
653 global scale, J. Geophys. Res., 116, D15109, doi:10.1029/2011JD015681, 2011.

654 Xie, L. H., Wei, G. J., Deng, W. F., and Zhao, X. L.: Daily $\delta^{18}\text{O}$ and δD of precipitations from
655 2007 to 2009 in Guangzhou, South China: Implications for changes of moisture sources, J.
656 Hydrol, 400, 477-489, 2011.

657 Yang, X. X., Yao, T. D., Yang, W. L., Xu, B. Q., He, Y., and Qu, D. M.: Isotopic signal of earlier
658 summer monsoon onset in the Bay of Bengal, J. Climate, 25, 2509-2515,
659 doi:10.1175/JCLI-D-11-00180.1, 2012.

660 Yuan, D. X., Cheng, H., Edwards, R. L., Dykoski, C. A., Kelly, M. J., Zhang, M. L., Qing, J. M.,
661 Lin, Y. S., Wang, Y. J., Wu, J. Y., Dorale, J. A., An, Z. S., and Cai, Y. J.: Timing, duration and
662 transition of the last interglacial Asian monsoon, Science, 304, 575-578, 2004.

663 Zhang, P. Z., Cheng, H., Edwards, R. L., Chen, F. H., Wang, Y. J., Yang, X. L., Liu, J., Tan, M.,
664 Wang, X. F., Liu, J. H., An, C. L., Dai, Z. B., Zhou, J., Zhang, D. Z., Jia, J. H., Jin, L. Y., and
665 Johnson, K. R.: A test of climate, sun, and culture relationships from an 1810-year Chinese
666 cave record, Science, 322, 940-942, 2008.